Influence of illumination-collection geometry on fluorescence spectroscopy in multilayer tissue

T. J. Pfefer[1] **L. S. Matchette**[1] **R. Drezek**[2]

[1]Center for Devices & Radiological Health, US Food & Drug Administration, Rockville, Maryland, USA
[2]Department of Bioengineering, Rice University, Houston, Texas, USA

Abstract—*Device–tissue interface geometry influences both the intensity of detected fluorescence and the extent of tissue sampled. Previous modelling studies have often investigated fluorescent light propagation using generalised tissue and illumination-collection geometries. However, the implementation of approaches that incorporate a greater degree of realism may provide more accurate estimates of light propagation. In this study, Monte Carlo modelling was performed to predict how illumination-collection parameters affect signal detection in multilayer tissue. Using the geometry and optical properties of normal and atherosclerotic aortas, results for realistic probe designs and a semi-infinite source-detection scheme were generated and compared. As illumination-collection parameters, including single-fibre probe diameter and fibre separation distance in multifibre probes, were varied, the signal origin deviated significantly from that predicted using the semi-infinite geometry. The semi-infinite case under-predicted the fraction of fluorescence originating from the superficial layer by up to 23% for a 0.2 mm diameter single-fibre probe and over-predicted by 10% for a multifibre probe. These results demonstrate the importance of specifying realistic illumination-collection parameters in theoretical studies and indicate that targeting of specific tissue regions may be achievable through customisation of the illumination-collection interface. The device- and tissue-specific approach presented has the potential to facilitate the optimisation of minimally invasive optical systems for a wide variety of applications.*

Keywords—*Fibre-optic probe, Fluorescence spectroscopy, Light–tissue interaction, Monte Carlo modelling, Optical diagnostics*

Med. Biol. Eng. Comput., 2004, **42**, 669–673

1 Introduction

MINIMALLY INVASIVE optical diagnostic techniques have undergone rapid development in recent years, leading to the emergence of numerous clinical devices for the detection of diseases such as cancer. One of the most promising optical approaches, fluorescence spectroscopy, has shown the ability to diagnose mucosal precancers in a variety of tissue sites with high levels of sensitivity and specificity (WAGNIERES *et al.*, 1998). However, for it to achieve widespread clinical acceptance, accuracy levels that equal or exceed those of existing diagnostic modalities will be required. Whereas much of the previous research in this field has involved optimisation of excitation and emission wavelengths, quantitative diagnostic algorithms and investigation of contrast agents, relatively little effort has been devoted to characterising the role of illumination-collection parameters and, particularly, their effect on spatial sampling of tissue.

Previous theoretical studies have provided some important insights into how optical device–tissue interface design affects fluorescence detection. These studies have often involved analyses of probes that incorporate optical fibres that transport light by total internal reflection. Several groups have shown that design parameters such as fibre-optic probe diameter and source–detector separation distance can influence the extent to which chromophores such as blood affect the spectral distribution of fluorescence (KEIJZER *et al.*, 1989; RICHARDS-KORTUM *et al.*, 1989; DACOSTA *et al.*, 1997; AVRILLIER *et al.*, 1998). The effect of fibre–sample separation distance and angular detection aperture on total detected fluorescence was predicted, using Monte Carlo modelling, to affect collection strongly (RICHARDS-KORTUM, 1995). Although a recent study by VISHWANATH *et al.* (2002) indicated that, for commonly used probe configurations, interface geometry had a relatively small effect on time-resolved fluorescence measurements, most previous studies on this subject have indicated that illumination-collection design has a variety of significant implications for optical diagnostics.

The extent to which individual tissue layers are interrogated during fluorescence diagnostics has been analysed theoretically for a few specific applications. In an early study, GMITRO *et al.* (1988) developed a simple Beer's law model of fluorescent light propagation to estimate measurement depth in arterial tissue. Several years later, a multilayer Monte Carlo model of fluorescent light propagation in arterial tissue was

Correspondence should be addressed to Dr T. Joshua Pfefer; email: tdp@cdrh.fda.gov

Paper received 19 November 2003 and in final form 15 March 2004
MBEC online number: 20043917

developed by WELCH *et al.* (1997) and used to generate novel information on the distribution of emission locations for detected photons. In other studies, Monte Carlo models have been used to investigate the fluorescence origin in normal and diseased bronchial (QU *et al.*, 1995) and colonic mucosa (ZONIOS *et al.*, 1996; DACOSTA *et al.*, 1997). Although these studies have produced significant insights into the origin of the fluorescence signal, none has provided a significant analysis of the effect of illumination-collection parameters on signal origin.

In recent years, our group and others have analysed the effect of device design on the fluorescence signal origin. In two initial studies, we used a Monte Carlo model to characterise the effect of specific parameters, such as optical-fibre diameter, numerical aperture, fibre-sample spacing and illumination-collection fibre separation distance, on spatial sensitivity to tissue fluorophores in a homogeneous turbid medium for single- (PFEFER *et al.*, 2001) and multiple- (PFEFER *et al.*, 2002) fibre geometries. Several of the trends found in these computational studies were subsequently verified through *in vitro* measurements of multilayer tissue phantoms (PFEFER *et al.*, 2003). A parametric analysis of fibre-optic probe designs was recently published by ZHU *et al.* (2003) using a two-layer tissue geometry based primarily on cervical epithelium. Although we are not aware of any experimental study that has rigorously analysed illumination-collection design for targeting of specific layers, a recent numerical investigation evaluated a variable-aperture method for estimating the distribution of fluorophores in tissue (QUAN and RAMANUJAM, 2002).

The present study was performed to improve understanding of fluorescent light propagation in layered tissue and to evaluate the concept of a device- and tissue-specific computational approach to optimising device design for specific layered-tissue applications. The primary goal of this study was to characterise the effect of illumination-collection parameters on the origin of fluorescence signals in layered tissue. Monte Carlo simulations performed for this study were based on the normal/atherosclerotic aorta paradigm implemented by WELCH *et al.* (1997) so as to enable comparisons with the earlier study.

2 Methods

Numerical modelling of light transport was performed using a modified version of the non-weighted photon Monte Carlo approach implemented previously (PFEFER *et al.*, 2001; 2002). This model now includes the option of specifying the thickness and optical properties of an arbitrary number of layers (WELCH *et al.*, 1997). The Monte Carlo method provides a simple, accurate and flexible, yet potentially time-consuming, method for investigating light–tissue interaction. Detailed explanations of the Monte Carlo technique are available in the literature (JACQUES and WANG, 1995; WANG *et al.*, 1995).

Photon launch was based on a uniform beam profile, with the launch angle uniformly distributed among angles within the cone specified by the equation $\theta_t = \sin^{-1}(NA/n_t)$, where θ_t is the cone half-angle, NA is the numerical aperture of the fibre, and n_t is the index of refraction of the tissue, which was set to 1.4 for all simulations. This equation was also used to determine the range of angles of fluorescence photons that were accepted by the detection scheme. Photons were propagated in three-dimensional space according to standard non-weighted photon Monte Carlo techniques. Absorption of an excitation photon was followed by isotropic emission of a fluorescence photon at the same location, thus producing a quantum efficiency of unity.

Each detected photon was binned in a two-dimensional array (r, z), according to its radial position at detection and depth of emission. The origin of this co-ordinate system was the centre of the illumination beam. Each bin was 0.025 mm thick in both the radial and axial (z) directions. This approach enables the user to generate signal origin distributions for a variety of detection regions from a single simulation. For any specific geometry, the depthwise emission distributions were calculated by multiplication of the number of detected fluorescence photons emitted at each bin depth by the local relative fluorescence coefficient and then normalisation of the distribution by the sum over all depths. The fluorescence coefficient was defined as the ratio of photons emitted in a small volume to the number of photons absorbed and thus accounted for quantum yield as well as absorption by non-fluorescent constituents.

The simulated tissue was represented by a cylinder 10 mm in diameter and 7.5 mm deep. The large simulated volume made it possible for any photons crossing out of the tissue to be terminated (except at the surface, where the standard optical laws of internal reflection were applied), without the detected signal being significantly affected. Data on optical properties and geometry are displayed in Table 1. The index of refraction of the tissue n_t was 1.4. The environmental index of refraction n_i was set to 1.45 to match that of the fibre-optic probe, except for two of the semi-infinite cases, when it was set to 1.0 to represent a tissue–air interface. All simulations were performed using 10^8 photons, so as to achieve convergence of the emission distributions.

The primary design parameters investigated in this study (as illustrated in Fig. 1) were single-fibre probe diameter D (or, for multifibre probes, illumination fibre diameter D_s and collection fibre diameter D_c) and illumination-collection fibre separation distance L. Note that L was defined as the edge-to-edge fibre separation distance, rather than centre-to-centre distance.

3 Results

A total of nine illumination-collection designs were investigated in this study: three single-fibre probes; two multifibre probes and four cases incorporating a semi-infinite collection geometry. The three single-fibre probe cases differed only in their diameter: 0.2, 0.6 and 1.0 mm. The multifibre probe cases were labelled MF_1 ($D_s = 0.2$ mm, $L = 0.05$ mm, $D_c = 0.2$ mm) and MF_2 ($D_s = 0.2$ mm, $L = 0.2$ mm, $D_c = 0.4$ mm). Probe MF_1 employed a small source-detection fibre separation and thus

Table 1 Tissue geometry and optical properties (absorption coefficient μ_a, scattering coefficient μ_s and scattering anisotropy g) used in simulations (WELCH et al. 1997). Tissue layers are listed according to spatial location, with most superficial layer listed first

			Excitation (476 nm)			Emission (600 nm)		
Tissue layer	Thickness, mm	Fluorescence coefficient	μ_a, cm^{-1}	μ_s, cm^{-1}	g, cm^{-1}	μ_a, cm^{-1}	μ_s, cm^{-1}	g, cm^{-1}
normal tissue								
intima	0.3	4.5×10^{-5}	7.5	240	0.85	3	170	0.84
media	0.85	8.2×10^{-5}	6.5	412	0.89	2	323	0.89
adventitia	0.25	5.5×10^{-5}	15	270	0.75	5	215	0.76
atherosclerotic tissue								
fibrous cap	0.5	2.8×10^{-5}	13	412	0.89	4	331	0.89
necrotic core	1.5	2.5×10^{-4}	6.5	412	0.89	2	331	0.89

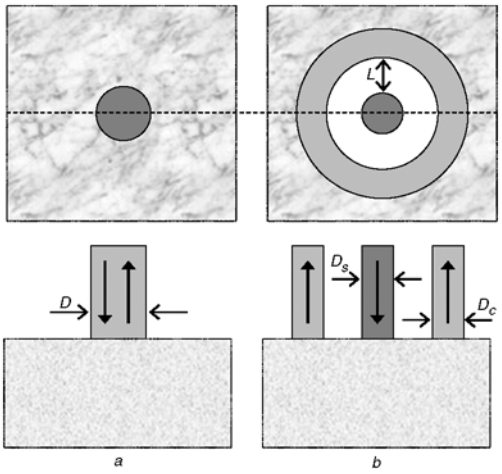

Fig. 1 *Top and cross-sectional views of (a) single-fibre and (b) multifibre probe geometries used in simulations*

should have provided optimum sensitivity to regions near the surface, whereas MF_2 employed a larger separation distance and larger detection fibres, which should have produced a more homogeneous interrogation of the tissue layers, based on the findings of our previous study (PFEFER *et al.*, 2002).

The primary semi-infinite case investigated here (SI case 1) was introduced previously by WELCH *et al.* (WELCH *et al.*, 1997) (and was labelled 'SI case 1') and involved illumination by a pencil beam and detection of all photons that exited the tissue surface. Detection of all photons was accomplished by setting the collection *NA* to a value of 1.4, thus producing a collection half-angle θ_t of 90°. Three other semi-infinite cases with slight variations were also simulated to illustrate the role of specific parameters.

Fluorescence origin distributions for several illumination-collection geometries in normal and atherosclerotic aortas are shown in Figs 2 and 3, respectively. These curves show a sharp increase in signal at the superficial edge of the second layer owing to changes in the fluorescence coefficient. Single-fibre probe data indicate a shift from high selectivity to the first layer for the $D = 0.2$ mm case to a more homogeneous probing with depth and a small subsurface peak in sensitivity as D increased. Both multifibre sensitivity profiles contain subsurface peaks 0.1–0.2 mm below the surface and display greater sensitivity to deeper layers than the single-fibre probes. In general, the trends seen in Fig. 3 are similar to those in Fig. 2. The primary differences are that, for atherosclerotic tissue, the location of the second layer was deeper, and there was a stronger decay in fluorescence with depth owing to the higher absorption coefficient of the necrotic core.

Data in Fig. 2 illustrate the large differences between results for semi-infinite and probe-based cases. Compared with SI case 1, the 0.2 mm single-fibre probe showed about twice as much relative sensitivity to the most superficial region of the intima and 60% less sensitivity to the most superficial region of the media. The multifibre probes indicated better agreement with SI case 1, and yet MF_2 still showed only half as much sensitivity to the most superficial region of the intima and 35% greater sensitivity in the most superficial region of the media. In terms of the percentage of detected fluorescence originating from the intima, the model predicted a value of 67% for SI case 1, whereas, for the 0.2 mm single-fibre and MF_2 probes, the predicted values were 90% and 57%, respectively. Similarly large differences between SI case 1 and these probe designs were seen for the atheromatous case in Fig. 3, with the percentage of detected fluorescence originating from the fibrous cap being 82% for SI case 1, 96% for the 0.2 mm single-fibre probe and 74% for the MF_2 probe.

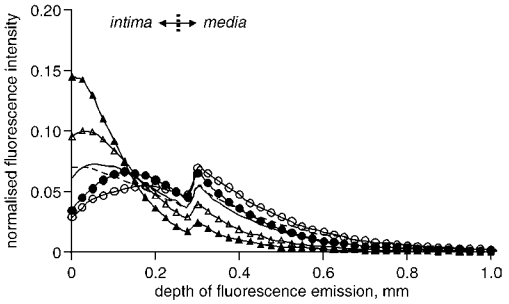

Fig. 2 *Simulation results demonstrating effect of illumination-collection parameters on interrogation of normal aorta. Graph contains data for three single-fibre cases, one SI case and two multifibre (MF) cases. Data were normalised to total detected fluorescence. As indicated, the intima-media boundary occurs at a depth of 0.3 mm. (–▲–) Single fibre, $D = 0.2$ mm. (–△–) Single fibre, $D = 0.4$ mm. (—) Single fibre, $D = 1.0$ mm. (– · – · –) SI case 1. (–●–) MF_1: $D_s = 0.2$ mm; $L = 0.05$ mm; $D_c = 0.2$ mm. (–○–) MF_2: $D_s = 0.2$ mm; $L = 0.2$ mm; $D_c = 0.4$ mm*

The results in Figs 2 and 3 indicated relatively good agreement between SI case 1 and the 1.0 mm single-fibre case. The similarities between these cases are surprising, given the significant differences in the illumination-collection parameters, specifically, the size and location of the source/detection regions, collection *NA* (0.22 against an unrestricted collection aperture) and the index of refraction of the environment (n_i of 1.45 against 1.0). To elucidate these results, three additional semi-infinite cases were analysed: these were identical to SI case 1, except that an n_i of 1.45 and/or a collection *NA* of 0.22 were implemented.

Sensitivity distributions for all four semi-infinite cases are displayed in Fig. 4. This graph indicates that changing n_i had a minimum effect for the semi-infinite cases (SI case 2). Changing *NA* from 1.4 to 0.22 (SI case 3) reduced relative sensitivity near the surface by 9%. When both parameters were changed from the SI case 1 levels to $NA = 0.22$ and $n_i = 1.45$ (SI case 4), a decrease of 38% was produced. The decrease in sensitivity to the superficial region when *NA* was changed to 0.22 was due to the loss of the ability to detect photons that were emitted at locations near the surface at angles outside the acceptance cone and that escaped the tissue without significant scattering. The difference in sensitivity distribution between SI cases 3 and 4 is due to the fact that, in the former case, photons emitted at shallow depths and angles outside the acceptance cone have a greater chance of being reflected back into the tissue and eventually detected, whereas, in the latter case, high-angle photons are more likely to exit the tissue and avoid detection. Therefore the combination of an unrealistic angular aperture and an air–tissue boundary condition produced a result very similar to that for a 1.0 mm diameter fibre.

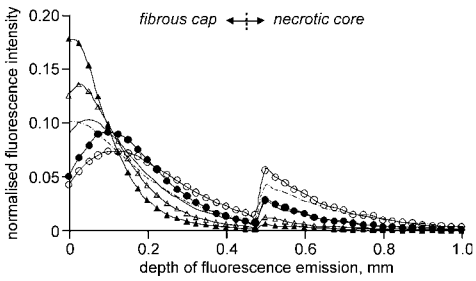

Fig. 3 *Simulation results demonstrating effect of illumination-collection parameters on interrogation of atherosclerotic aorta. (–▲–) Single fibre, $D = 0.2$ mm. (–△–) Single fibre, $D = 0.4$ mm. (—) Single fibre, $D = 1.0$ mm. (– · – · –) SI case 1. (–●–) MF_1: $D_s = 0.2$ mm; $L = 0.05$ mm; $D_c = 0.2$ mm. (–○–) MF_2: $D_s = 0.2$ mm; $L = 0.2$ mm; $D_c = 0.4$ mm*

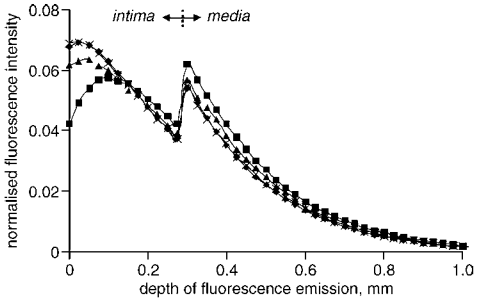

Fig. 4 *Simulation results for SI geometries documenting role of n_i and NA_c on interrogation of normal aorta. Note that NA_c refers to numerical aperture of collection scheme. (–×–) SI case 1 ($n_i = 1.0$, $NA_c = 1.4$); (–♦–) SI case 2 ($n_i = 1.45$, $NA_c = 1.4$); (–▲–) SI case 3 ($n_i = 1.0$, $NA_c = 0.22$); (–■–) SI case 4 ($n_i = 1.45$, $NA_c = 0.22$)*

It is worth noting that Fig. 4 also provides insight into probe or imaging-based device designs in which the detection region is much larger than the illumination beam. For such designs, our model indicates that an increase in sensitivity of about 20% to tissue regions within 0.1 mm of the surface can occur when there is a significant index mismatch at the surface, compared with a matched boundary condition (SI case 4).

Total detected fluorescence levels are presented in Fig. 5 as a function of illumination-collection geometry and tissue type. Signal levels for SI cases 1 and 2 were much higher than all others owing to much larger NAs. The increase in detected signal with fibre diameter in single-fibre probes and with detection area in multifibre probes was consistent with our previous studies. Whereas a 0.2 mm diameter single fibre was predicted to collect relatively low levels of fluorescence, it may be possible to double the detected signal level by implementing two fibres in a single probe. Monte Carlo simulations indicate that, if these two fibres are separated by 0.5 mm (edge-to-edge distance), with both used simultaneously for illumination and collection, only 3% of the fluorescence detected by each fibre would be due to excitation light originating from the other fibre. This level of isolation would ensure that depthwise emission distributions would not change significantly from the single-fibre case.

Results in Fig. 5 indicate that the difference in the detected signal between tissue types is greatest for the semi-infinite cases and increases with fibre diameter for single-fibre probes. For multifibre probes, the design with larger fibre diameter and separation distance produced the greatest differences. These trends indicate that difference in signal was a function of photon pathlength (PFEFER *et al.*, 2002) and probably due to the higher absorption level in atheromatous tissue at both excitation and emission wavelengths.

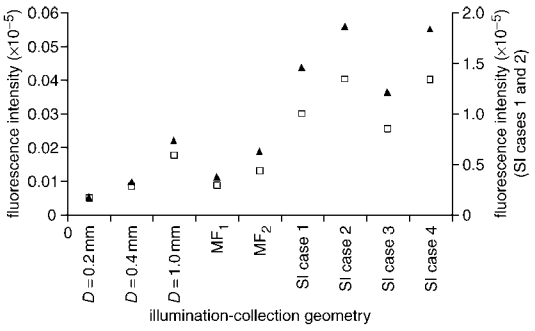

Fig. 5 *Detected fluorescence signal intensity as function of illumination-collection geometry in (▲) normal and (□) atherosclerotic aortas. Note that first three cases represent single-fibre probes. Secondary axis (right side) applies to SI cases 1 and 2 only*

4 Discussion

Theoretical and experimental studies of illumination-collection design have begun to provide important insights into issues relevant to light propagation in biological tissue during fluorescence diagnostic procedures. In our earlier publications, we focused on generalised cases to illustrate the effect of specific device parameters. The present study represents an initial effort to address the role of interface design using a multilayered model that simulates the morphology and optical properties of a specific tissue. It should be noted that, although we have previously investigated multifibre probes with various probe–tissue spacer sizes, such cases are not included in this study, as results indicated that, as spacer size increases, the sensitivity distribution changes from a typical multifibre probe distribution (subsurface peak) to a distribution more reminiscent of a large single-fibre probe (surface or near-surface peak).

The present study is strongly based on a seminal article by WELCH *et al.* (1997), in which the authors used a layered-tissue Monte Carlo model to analyse the propagation of light during fluorescence-based interrogation of the aorta. Results from this earlier study provided novel insight into the origin of detected signals in normal and atherosclerotic tissue. However, these simulations involved an illumination-collection geometry that was not based on realistic device designs: pencil beam illumination and detection of any fluorescence escaping from the tissue surface, regardless of angle. Our study showed a surprising result: that the Welch *et al.* case provided a level of interrogation that was very similar to that of a 1.0 mm diameter single-fibre probe. This result was unexpected, because the 1.0 mm probe case had a different size and shape of source and detector, a restriction on the angular acceptance angle of fluorescence photons and a different boundary condition (fibre–tissue as opposed to air–tissue). Our findings indicate that the effects of these different parameters cancel each other out to some extent, which led to the unexpected similarity in results.

There are several potential pitfalls when using a single, generalised case to describe signal origin, particularly when a non-physical situation is implemented. Although there was good agreement between the 1.0 mm and semi-infinite cases in Figs 2 and 3, the overall detected signal predicted for the latter was much larger than that predicted for the former. Also, when a different set of optical properties is implemented, the agreement between the probe and semi-infinite cases may not be as good. Thirdly, the use of a single illumination-collection design does not provide a thorough picture of the range of signal origin distributions that can be achieved.

Perhaps the optimum way to summarise the range of possibilities is with several bounding cases, such as large and small single-fibre probes, multifibre probes with small and large lateral fibre separation distances and possibly a semi-infinite case and/or imaging geometry. Although simulating five or six cases is more labour-intensive than a single case, a much more thorough description will be achieved.

By varying illumination-collection parameters, we found several trends that showed a strong similarity to those found in our previous studies of homogeneous media. The diameter of single-fibre probes strongly influenced signal origin, with smaller diameters causing strong selectivity for highly superficial regions, and larger diameters producing a more homogeneous interrogation of the tissue. The larger single-fibre geometries in the present study showed more of a subsurface peak in sensitivity than in our previous study, probably owing to a higher absorption coefficient. The multifibre probes also produced subsurface detection peaks, but probed the tissue in a more homogeneous manner. As fibre separation distance increased for these multifibre probes, as expected, there was

an increase in the relative increase in signal detected from secondary layers.

In previous studies that analysed fluorescent light propagation in colonic (ZONIOS *et al.*, 1996) and cervical (DREZEK *et al.*, 2001) tissue, it was suggested that isolating signals originating from individual layers could enhance detection of neoplasia. The potential to optimise device design for targeting specific tissue regions is supported by the present study.

The results of this study provide insights into specific ways to optimise probe design for the detection of atherosclerosis. For example, using a small, single-fibre probe would enable more selective interrogation of the fibrous cap, the thickness of which may be correlated with plaque instability (ARAKAWA *et al.*, 2002). The use of a multifibre probe would maximise the relative signal detected from deeper layers, or a combination of illumination-collection arrangements could target tissue regions at different depths so as to optimise measurement of the spectral and/or temporal fluorescence characteristics of individual layers. If signal maximisation was a priority, Fig. 5 indicates that the use of a larger single-fibre probe or a multifibre probe with a large collection region would be most appropriate.

5 Conclusions

By building on a previous investigation by WELCH *et al.* (1997), we have reached several conclusions that help to elucidate basic fluorescent light propagation phenomena and may lead to improvements in disease detection. Our computational results support the idea that it is necessary to implement realistic device–tissue interface parameters in theoretical analyses to provide a thorough and accurate description of light propagation and signal origin. The illumination-collection geometry, particularly fibre diameter and illumination-collection fibre separation distance, was shown to affect the way in which a fibre-optic probe interrogates multilayer turbid tissues.

Although experimental data are necessary to evaluate the potential to optimise detection of atherosclerotic lesions, the data presented here indicate the potential to optimise the design of fluorescence-based devices for the targeting of tissue layers. Finally, this study also demonstrates that Monte Carlo modelling is a useful tool for estimating fluorescent light propagation in arbitrary multilayer turbid tissues and may play a key role in the development of more accurate, tissue-specific, optical diagnostic devices.

References

ARAKAWA, K., ISODA, K., ITO, T., NAKAJIMA, K., SHIBUYA, T., and OHSUZU, F. (2002): 'Fluorescence analysis of biochemical constituents identifies atherosclerotic plaque with a thin fibrous cap', *Arterioscler. Thromb. Vasc. Biol.*, **22**, pp. 1002–1007

AVRILLIER, S., TINET, E., ETTORI, D., TUALLE, J. M., and GELEBART, B. (1998): 'Influence of the emission-reception geometry in laser-induced fluorescence spectra from turbid media', *Appl. Opt.*, **37**, pp. 2781–2787

DACOSTA, R. S., LILGE, L. D., KOST, J., CIRROCO, M., HASSARAM, S., MARCON, N., and WILSON, B. C. (1997). 'Confocal fluorescence microscopy, microspectrofluorimetry, and modeling studies of laser-induced fluorescence endoscopy (LIFE) of human colon tissue', *Proc. SPIE*, **2975**, pp. 98–107

DREZEK, R., SOKOLOV, K., UTZINGER, U., BOIKO, I., MALPICA, A., FOLLEN, M., and RICHARDS-KORTUM, R. (2001): 'Understanding the contributions of NADH and collagen to cervical tissue fluorescence spectra: modeling, measurements, and implications', *J. Biomed. Opt.*, **6**, pp. 385–396

GMITRO, A. F., CUTRUZZOLA, F. W., STETZ, M. L., and DECKELBAUM, L. I. (1988): 'Measurement depth of laser-induced fluorescence with application to laser angioplasty', *Appl. Opt.*, **27**, pp. 1844–1849

JACQUES, S. L., and WANG, L. (1995): 'Monte Carlo modeling of light transport in tissues', in WELCH, A. J., and VAN GEMERT, A. J. (Eds): 'Optical-thermal response of laser-irradiated tissue' (Plenum Press, New York, 1995)

KEIJZER, M., RICHARDS-KORTUM, R. R., JACQUES, S. L., and FELD, M. S. (1989): 'Fluorescence spectroscopy of turbid media: autofluorescence of the human aorta', *Appl. Opt.*, **28**, pp. 4286–4292

PFEFER, T. J., SCHOMACKER, K. T., EDIGER, M. N., and NISHIOKA, N. S. (2001): 'Light propagation in tissue during fluorescence spectroscopy with single-fiber probes', *IEEE J. Sel. Top. Quant. Elect.*, **7**, pp. 1004–1012

PFEFER, T. J., SCHOMACKER, K. T., EDIGER, M. N., and NISHIOKA, N. S. (2002): 'Multiple-fiber probe design for fluorescence spectroscopy in tissue', *Appl. Opt.*, **41**, pp. 4712–4721

PFEFER, T. J., MATCHETTE, L. S., ROSS, A. M., and EDIGER, M. N. (2003): 'Selective detection of fluorophore layers in turbid media: the role of fiberoptic probe design', *Opt. Lett.*, **28**, pp. 120–122

QU, J., MACAULAY, C., LAM, S., and PALCIC, B. (1995): 'Laser-induced fluorescence spectroscopy at endoscopy: tissue optics, Monte Carlo modeling and *in vivo* measurements', *Opt. Eng.*, **34**, pp. 3334–3343

QUAN, L., and RAMANUJAM, N. (2002): 'Relationship between depth of a target in a turbid medium and fluorescence measured by a variable-aperture method', *Opt. Lett.*, **27**, pp. 104–106

RICHARDS-KORTUM, R., MEHTA, A., HAYES, G., COTHREN, R., KOLUBAYEV, T., KITTRELL, C., RATLIFF, N. B., KRAMER, J. R., and FELD, M. S. (1989): 'Spectral diagnosis of atherosclerosis using an optical fiber laser catheter', *Am. Heart J.*, **118**, pp. 381–391

RICHARDS-KORTUM, R. (1995). 'Fluorescence spectroscopy of turbid media', in WELCH, A. J., and VAN GEMERT, M. J. C. (Eds): 'Optical-thermal response of laser-irradiated tissue' (Plenum Press, 1995)

VISHWANATH, K., POGUE, B. W., and MYCEK, M. A. (2002): 'Quantitative fluorescence lifetime spectroscopy in turbid media: comparison of theoretical, experimental and computational methods', *Phys. Med. Biol.*, **47**, pp. 3387–3405

WAGNIERES, G. A., STAR, W. M., and WILSON, B. C. (1998): '*In vivo* fluorescence spectroscopy and imaging for oncological applications', *Photochem. Photobiol.*, **68**, pp. 603–632

WANG, L., JACQUES, S. L., and ZHENG, L. (1995): 'MCML — Monte Carlo modeling of light transport in multi-layered tissues', *Comput. Methods Programs Biomed.*, **47**, pp. 131–146

WELCH, A. J., GARDNER, C., RICHARDS-KORTUM, R., CHAN, E., CRISWELL, G., PFEFER, J., and WARREN, S. (1997): 'Propagation of fluorescent light', *Lasers Surg. Med.*, **21**, pp. 166–178

ZHU, C., LIU, Q., and RAMANUJAM, N. (2003): 'Effect of fiber optic probe geometry on depth-resolved fluorescence measurements from epithelial tissues: a Monte Carlo simulation', *J. Biomed. Opt.*, **8**, pp. 237–247

ZONIOS, G. I., COTHREN, R. M., ARENDT, J. T., WU, J., VAN DAM, J., CRAWFORD, J. M., MANOHARAN, R., and FELD, M. S. (1996): 'Morphological model of human colon tissue fluorescence', *IEEE Trans. Biomed. Eng.*, **43**, pp. 113–122

Authors' biographies

T. JOSHUA PFEFER received a PhD in biomedical engineering (1999) from the University of Texas at Austin. He completed postdoctoral fellowships at Massachusetts General Hospital and the U.S. Food and Drug Administration, where he is the Optical Diagnostics and Therapeutics Laboratory Leader.

REBEKAH DREZEK received her PhD in electrical engineering from the University of Texas at Austin. She joined Rice University in 2002 where she is currently the Stanley C. Moore Assistant Professor of Bioengineering.

L. STEPHANIE MATCHETTE joined the National Institute for Occupational Safety and Health in 1977 and FDA/CDRH as a Research Chemist in 1981. Her investigative experience includes studies of DNA replication, UV and chemical mutagenesis, and polymer toxicology.